Fluorescence-based characterisation of selected edible insect species: Excitation emission matrix (EEM) and parallel factor (PARAFAC) analysis

G. Rossi [a], J. Durek [a], S. Ojha [a], O.K. Schlüter [a,b,*]

[a] *Quality and Safety of Food and Feed, Leibniz Institute for Agricultural Engineering and Bioeconomy (ATB), Max-Eyth-Allee 100, 14469, Potsdam, Germany*
[b] *Department of Agricultural and Food Sciences, University of Bologna, Piazza Goidanich 60, 47521, Cesena, Italy*

ARTICLE INFO

ABSTRACT

Fluorescence spectroscopy coupled with chemometric tools is a powerful analytical method, largely used for rapid food quality and safety evaluations. However, its potential has not yet been explored in the novel food sector. In the present study, excitation emission matrices (EEMs) of 15 insect powders produced by milling insects belonging to 5 Orthoptera species (*Acheta domesticus, Gryllus assimilis, Gryllus bimaculatus, Locusta migratoria, Schistocerca gregaria*) from 3 different origins were investigated. Parallel factor (PARAFAC) analysis performed on the overall averaged dataset was validated for five components, highlighting the presence of five different fluorescence peaks. The presence of these peaks was confirmed on each species, suggesting that fluorescence compounds of edible insects are the same in several species. PARAFAC analysis performed on the overall averaged dataset after alternatively adding the EEM recorded from one standard compound allowed to speculate that edible insects fluorescence raises from mixtures of: tryptophan + tyrosine (PARAFAC component-1), tryptophan + tyrosine + tocopherol (PARAFAC component-2), collagen + pyridoxine + pterins (PARAFAC component-3). This study suggests that fluorescence spectroscopy may represent a powerful method for investigating composition and quality of insect-based foods.

1. Introduction

Edible insects represent a very interesting trend in the food sector as they can grow on waste and by-products, converting them into materials rich in nutrients (Bosch et al., 2019; Gasco et al., 2020; Ojha et al., 2020; Pinotti et al., 2019). As their consumption spreads in developed countries, an increasing number of companies show interest in their production and transformation. However, due to the particular nature of this new food, accurate quality evaluation should always be performed in order to prevent unexpected quality changes for the consumers and economic and legal issues for the producers.

Traditional analytical techniques are destructive, time-consuming and need strong knowledge support (Hassoun et al., 2020), making them difficult for industrial applications. Innovative, fast and alternative methods include spectroscopic tools such as fluorescence spectroscopy, (Fourier Transformed) infrared spectroscopy, X-ray spectroscopy, Raman spectroscopy, nuclear magnetic resonance and others. These are characterised by rapidity and no need of sample preparation, making them suitable for in-line quality monitoring (Andersen and Mortensen,

2008; He and Sun, 2015; Li and Church, 2014; Patra, 2003; Porep et al., 2015; Silva et al., 2020). Among these, fluorescence is a very attractive technique because it appears to be 100–1000 times more sensitive than other spectroscopic methods (Albani, 2012; Strasburg and Ludescher, 1995), allowing a wide range of analyses in short time (Hassoun et al., 2020). Fluorescence landscape, also known as optical fingerprint or excitation emission matrix (EEM) is a tridimensional representation (i.e. three-way array) of the fluorescence spectra of one sample, which is recorded over several excitation and emission wavelengths. It describes the overall fluorescence pattern of the sample, allowing to perform a comprehensive chemical and physical characterisation of the product (Andrade-Eiroa et al., 2013). However, due to the extreme complexity of biological samples, along with some phenomena as quenching and interaction among several compounds, interpretation of EEM may be challenging (Elcoroaristizabal et al., 2015), requiring the use of powerful chemometric tools, such as PARAllel FACtor (PARAFAC) analysis (Andrade-Eiroa et al., 2013; Lenhardt et al., 2015).

PARAFAC is a decomposition method based on alternating least square (ALS) algorithm, which allows to visualise the EEM as the sum of

---

several fluorescence compounds (fluorophores) present in the analysed sample (Bro, 1997). It has already been used to characterise complex mixtures and discriminate several biological matrices, as well as foods and drinks (Acković et al., 2018; Lenhardt et al., 2017; Sikorska et al., 2019; Stedmon and Bro, 2008; Stedmon and Markager, 2005; Wunsch et al., 2017; Yamashita et al., 2008). However, its potential is still poorly explored in the novel food sector (Khan et al., 2019; Millie et al., 2002).

Therefore, the aim of this study was to characterise the recorded fluorescence landscape of 15 edible insect powders from 5 different species. PARAFAC function was implemented on overall and intraspecies EEMs and further identification of the fluorescence compounds was performed.

2. Materials and methods

2.1. Insects

Live adult insects from 5 Orthoptera species, three belonging to Ensifera suborder (*Acheta domesticus* L., *Gryllus assimilis* L., *Gryllus bimaculatus* D.G.) and two to Caelifera suborder (*Locusta migratoria* L., *Schistocerca gregaria* F.), were purchased from 3 local shops: Feeders and More GmbH (Au in der Hallertau, Germany), ProInsects GmbH (Minden, Germany), Tropic Shop (Nordhorn, Germany).

Live insects were separated from their feed by sieving and kept at their optimal growth conditions for 24 h in order to empty their gut. Temperature and humidity were selected according to data given in literature (Table 1). Subsequently, insects were inactivated by chilling at 4 °C for 1 h followed by freezing at −20 °C for 1 day and stored at −30 °C. Frozen samples were freeze-dried (Alpha 1–4 LSCplus, Martin Christ Gefriertrocknungsanlagen GmbH, Osterode am Harz, Germany) for 3 days at −58 °C and 600 mbar and ground with a knife mill (Grindomix GM200, Retsch GmbH, Haan, Germany) at 10 rpm, applying 2 cycles of 30 s, separated by a break of 30 s to homogenize the bulk. Afterwards, insect powders were stored at −20 °C until fluorescence analyses.

2.2. Chemicals

Based on fluorescence peaks recorded from the insect powders, fourteen chemical compounds were selected and investigated (Table 2). Pure standards ($\geq$98%) were purchased from Sigma-Aldrich (St. Louis, Missouri, USA) and Carl Roth GmbH (Karlsruhe, Germany) and used without further purification. Albumin, collagen, NADH, para-aminobenzoic acid, riboflavin, thiamin and tyrosine were analysed as powder in front-face mode. Stock solutions (1 g/L) of cobalamin, pterins, pyridoxine and tryptophan were prepared by singularly dissolving each standard in Milli-Q water, while retinol, tocopherol and tyramine were dissolved in ethanol (HPLC degree $\geq$99.5%; Carl Roth GmbH). Additionally, in order to investigate quenching and changes in fluorescence peak due to the interaction between compounds, mixtures

Table 1
Environmental conditions (temperature, relative humidity and photoperiods) used for fasting (24 h) of the studied insect species.

Species	Temperature (°C)	Relative humidity (%)	Photoperiods (hours; L:D)	Reference
Acheta domesticus	29 ± 1	65 ± 5	12:12	Oonincx et al. (2015)
Gryllus assimilis	27 ± 1	65 ± 5	12:12	Bertram and Rook (2011)
Gryllus bimaculatus	27 ± 1	60 ± 10	8:16	Song et al. (2016)
Locusta migratoria	30 ± 2	75 ± 5	16:8	Tu et al. (2012)
Schistocerca gregaria	30 ± 2	50 ± 5	12:12	Maeno et al. (2020)

Table 2
Chemical compounds and position of their maximum fluorescence peak selected for investigation of edible insect fluorescence landscape.

Chemical compound	Fluorescence Peak ($\lambda_{ex/em}$; nm)	References
Collagen	335/390; 370/460	Egelandsdal et al. (2005)
Pterins	345/425	Abels and Ludescher (2003)
Retinol	325/470	Duggan et al. (1957)
Tryptophan	280/350; 295/350	Moller and Denicola (2002)
Tyrosine	270/320; 275/300	Poveda et al. (2003); Yang et al. (2017)
Albumin	280/340	Bi et al. (2005)
Tocopherol	290/330	Zandomeneghi et al. (2005)
Thiamin (vit. B1)	370/460	Yang et al. (2016)
Riboflavin (vit. B2)	270/525; 370/525; 450/525	Yang et al. (2016)
Pyridoxin (vit. B6)	250/370; 325/370	Yang et al. (2016)
Cobalamin (vit. B12)	250/337	Pourreza et al. (2017)
NADH	335/414-438	Dufour et al. (2003)
p-aminobenzoic acid	295/345	Duggan et al. (1957)
Tyramine	275/310	Duggan et al. (1957)

of tryptophan (10 mg/l) and tyrosine (1 g/l) dissolved in Milli-Q water, tryptophan (0.1 g/l) and tocopherol (1 g/l) dissolved in ethanol, tyrosine (1 g/l) and tocopherol (1 g/l) dissolved in ethanol, tryptophan (0.1 g/l), tyrosine (0.7 g/l) and tocopherol (0.07 g/l) dissolved in ethanol, were prepared.

After dissolving, each solution was homogenized by stirring for 60 min at 1000 rpm. Subsequently, individual operative solutions with a concentration ranged between 10 mg/L and 1 g/L were prepared. Each solution was stored at 5 °C for 48 h prior to fluorescence analysis.

2.3. Fluorescence measurement

Fluorescence analyses of powdered insects and standards were carried out with a Perkin-Elmer LS55 Luminescence Spectrometer (Perkin-Elmer, Waltham, MA, USA) controlled by FL WinLab Perkin-Elmer 403 software. A pulsed xenon lamp set at 770 V and a red-sensitive photomultiplier (R928) were used as excitation source and emission detector, respectively. Insect powders, as well as powders of standard compounds, were analysed in front-face mode (Cell-holder nr. 52123130, Perkin-Elmer) using the multi-scan application and an incident angle of 60°. The illuminated area of the front-face cuvette was 7 mm high and 3 mm wide. Analyses of standard solutions were performed in 1 mm path-length acrylic transparent cuvettes (Sarstedt AG & Co., Nümbrecht, Germany) by using the standard single position Cell-holder (L2250140, Perkin-Elmer). Analysis of solvents (blank) was performed with the same setting and using the same cuvettes before the standard solutions were analysed. Insect powders were allowed to reach room temperature in the dark for 12 h before the analysis.

Fluorescence landscapes were obtained by scanning the emission spectra from 260 to 700 nm with steps of 1 nm, over excitation ranged between 240 and 600 nm in 5 nm steps. Excitation and emission monochromator slit widths were set at 10 nm and 2.5 nm, respectively. FGL280S Long-pass filter (Thorlabs, Newton, NJ, USA) was used as emission filter, while FGUV5S Band-pass filter (Thorlabs, Newton, NJ, USA) and FGS900S Long-pass filter (Thorlabs, Newton, NJ, USA) were the excitation filters used within the excitation interval 240–345 nm and 350–600 nm, respectively. All the measurements were performed at room temperature (20 ± 2 °C) and with an integration time of 0.06 s (scan speed = 500 nm/min). The data detected were mean-centred, block averaged, rationed and corrected for rhodamine reference cell. Each sample was scanned in triplicate and three independent spectra for each sample were obtained.

Raman peak was recorded by scanning Milli-Q water contained in a 10 mm cuvette at excitation 350 nm and emission ranged between 370

and 500 nm. Raman scan was performed in triplicate, and the three scans were mediated.

2.4. Data pre-processing

Recorded data (Raman spectra, samples spectra and blank) were read in Microsoft Excel (2010) (Microsoft Corporation, Albuquerque, NM, USA) and organized in order to have the overall spectra for each sample in one file.

In order to remove the specifics of the instrument and obtain correct, reproducible and easier to analyse EEMs, data were pre-processed through filter correction, Raman normalization and Rayleigh scatter deletion. Moreover, blank subtraction and inner filter effect correction were performed on filter corrected data for standard solutions in order to consider and delete the signals due to the solvents.

Filter correction was carried out by multiplying the recorded value with the percentage of transmission provided by the filters' manufacturer. Raman normalization was performed by dividing the fluorescence value through the area under the Raman peak, computed by integrating the filter corrected fluorescence signal recorded on Milli-Q water at excitation of 350 nm and emission between 371 and 428 nm (Lawaetz and Stedmon, 2009). Rayleigh first and second order scatter removal was performed by deleting the values at emission = excitation ±20 nm (Rayleigh first order scatter) and emission = [2 x excitation] ± 20 nm (Rayleigh second order scatter). Deleted data at Rayleigh first order scatter were treated as missing value (Andersen and Bro, 2003), while data at the Rayleigh second order scatter were replaced by interpolation (Elcoroaristizabal et al., 2015). Finally, scatter removed matrices were reduced by deleting noisy data and redundant information as addressed by plotting the EEMs. Therefore, data recorded at excitation higher than 530 nm and emission higher than 550 nm were deleted (Bugden et al., 2008).

Inner filter effect correction was performed for standard solutions by multiplying the EEMs by a correction matrix, which was calculated for each wavelength pair from the sample absorbance, recorded in triplicate with a Perkin-Elmer Lambda 950 UV-VIS/NIR spectrometer by assuming excitation and emission pathlengths of 0.5 cm in a 10 mm quartz cuvette (Ohno, 2002).

Filter correction, blank subtraction and inner filter correction were performed on Microsoft Excel 2010, while Raman normalization and Rayleigh scatter removal were carried out on MatLab R2019a (The MathWorks Inc., Natick, MA, USA), using drEEM toolbox version 0.6.3 (Murphy et al., 2013).

2.5. Chemometric analysis

PARAFAC analyses were implemented on the corrected data by using drEEM toolbox (Murphy et al., 2013), version 0.6.3, run under MatLab R2019a (The MathWorks Inc., Natick, MA, USA) statistical environment. Different datasets were prepared and submitted to the PARAFAC function. In a first step, each species was analysed separately in order to address potential differences between species. Afterwards, the three replicates from the same sample were averaged and PARAFAC function was implemented on the overall averaged dataset, consisting of 15 independent spectra (5 species x 3 shops). In this way, an overview of the complete EEMs of several insects belonging to the Orthoptera order could be obtained. In a further step, the three EEMs recorded on each standard solution were averaged and studied. Identification and attribution of each peak was performed by evaluating the improvements of the PARAFAC models built on the overall averaged dataset after alternating adding the EEM recorded by each standard compound.

If the insect powders are containing the studied standard compounds, core consistency and percentage of explained variance of the new PARAFAC models should not be significantly different when compared to the ones of the PARAFAC models computed on the original dataset.

Before running the PARAFAC function, each dataset was scaled on sample mode and normalized at unit of variance. Nine PARAFAC models, with a number of components ranged between 2 and 10, were built on each dataset by using the non-negative constraints on excitation and emission modes (Andersen and Bro, 2003). Convergence criteria, number of replications calculated to fix the models and maximum number of iterations were set at 10^{-6}, 10 and 2500, respectively. Core consistency diagnostic, percentage of explained variance and split-half analysis in 3 alternating and random splits were used to select and validate the right model (Stedmon and Bro, 2008).

3. Results

3.1. Fluorescence landscape

The corrected and reduced fluorescence landscape (excitation 240–530 nm; emission 260–550 nm), obtained by averaging three independent scans of the same insect powder, is shown in Fig. 1.

Each EEM is relative to one species purchased from one German seller. In every sample, a strong peak was detected in the region at excitation about 290 nm and emission about 330 nm. The intensity of this peak was highly variable among species and origins. Orthoptera suborder Ensifera (*Acheta domesticus*, *Gryllus assimilis*, *Gryllus bimaculatus*) displayed higher peak than Orthoptera suborder Caelifera (*Locusta migratoria*, *Schistocerca gregaria*), independently by the shop where the insects were bought. By considering several sellers, higher peak was detected on insects purchased by Feeders and More GmbH for all the studied species.

A prominent peak at $\lambda_{ex/em}$ around 340/430 nm was detected on *Locusta migratoria* from Tropic Shop, although the same peak could also be observed in the other samples. However, the aforementioned peak was not evident in samples other than *Locusta migratoria*. In all the samples, a clear peak was detected around excitation 340 nm and emission 395–400 nm. This peak was particularly evident in *Acheta domesticus* from Feeders and More GmbH. It was high in the other samples as well, although it was lower than the peak 340/430 nm ($\lambda_{ex/em}$) in *Gryllus bimaculatus* from Feeders and More GmbH. Further, a sharp peak was observed at $\lambda_{ex/em}$ of 355/460 nm in *Gryllus bimaculatus* from ProInsects GmbH, while powder of *Locusta migratoria* from the same shop was characterised by a peak at 355/420 nm ($\lambda_{ex/em}$). In powders of *Acheta domesticus*, *Gryllus assimilis* and *Locusta migratoria* from ProInsects GmbH and Tropic Shop, a weak peak was detected in the region 385–390/440-460 nm ($\lambda_{ex/em}$), while a peak at 335/390 nm ($\lambda_{ex/em}$) was noticed in *Schistocerca gregaria* from Feeders and More GmbH.

3.2. PARAFAC analysis

Core consistency and percentage of explained variance of PARAFAC models built on the averaged data recorded on the insect powders are displayed in Fig. 2. Core consistency shows a uniform decreasing trend, with a rapid fall between 4 (core consistency = 92.06%) and 5 components (core consistency = 67.91%) and between 6 (core consistency = 40.31%) and 7 components (core consistency = 7.56%). According to the core consistency, the percentage of explained variance raises from 96.54% (model-2) to 99.90% (model-10), with an important increment from 2 to 3 components (98.44%) and from 3 to 4 components (99.38%). Smaller increments were detected between 4, 5 (99.70%) and 6 (99.76%) components. Split-half analysis performed on the PARAFAC model with 4 and 5 components was validated on all the comparisons, while the same analysis carried out on model-6 was not validated (supplementary material S1).

Loadings of each component of the PARAFAC models 4, 5 and 6 described on sample, excitation and emission modes, are displayed in Fig. 3. Fluorescence peaks centred at $\lambda_{ex/em}$ 295/300 nm with shoulder at 333 nm (component blue), 285/333 nm (component orange) and 340/390–400 nm with shoulder at 420–425 nm (component yellow)
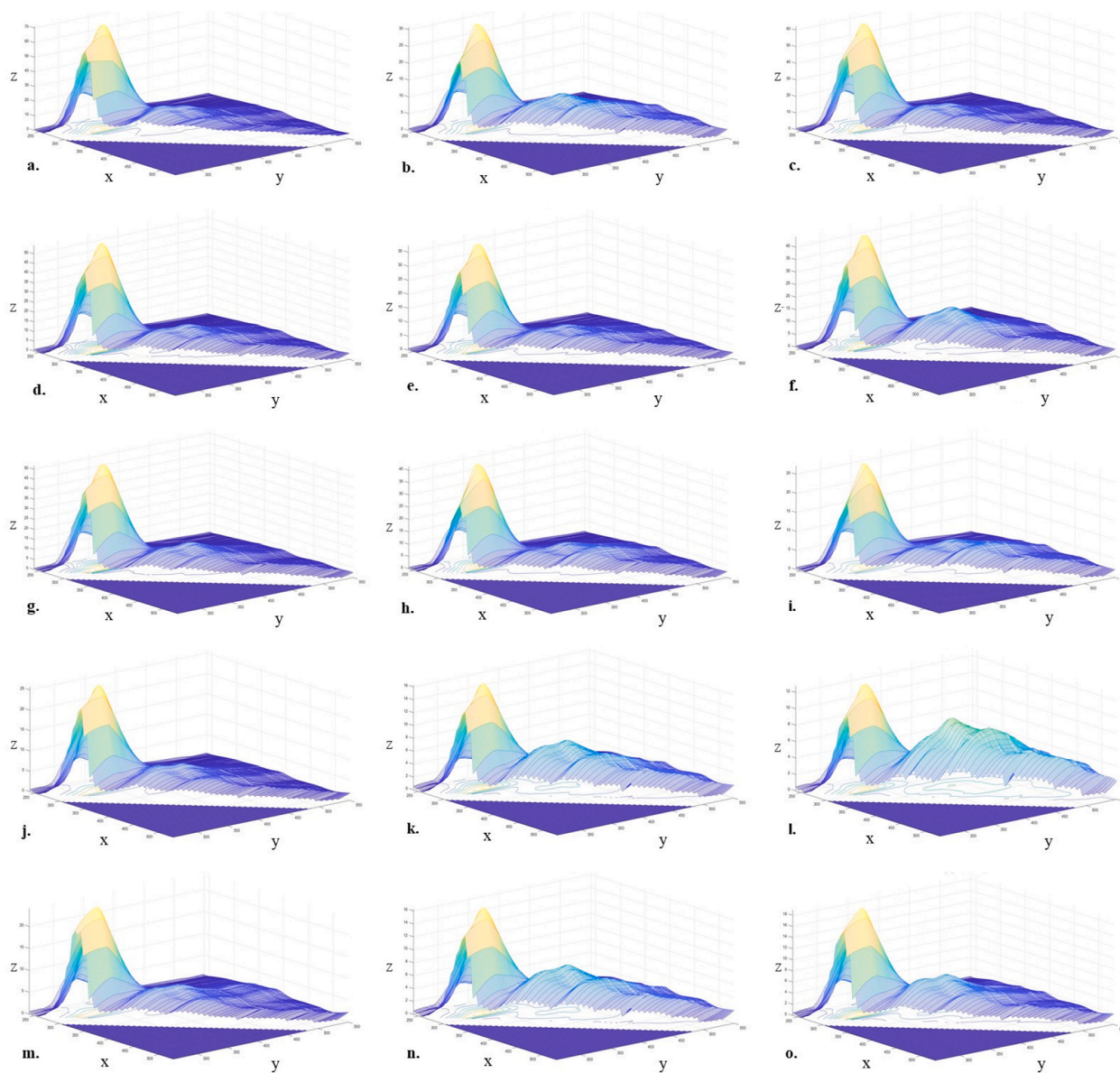
Fig. 1. Reduced, averaged and corrected fluorescence landscape recorded from the analysed samples: *Acheta domesticus* from: Feeders and More GmbH (a), ProInsects GmbH (b), Tropic Shop (c); *Gryllus assimilis* from: Feeders and More GmbH (d), ProInsects GmbH (e), Tropic Shop (f); *Gryllus bimaculatus* from: Feeders and More GmbH (g), ProInsects GmbH (h), Tropic Shop (i); *Locusta migratoria* from: Feeders and More GmbH (j), ProInsects GmbH (k), Tropic Shop (l); *Schistocerca gregaria* from: Feeders and More GmbH (m), ProInsects GmbH (n), Tropic Shop (o). X axis, excitation (nm); Y axis, emission (nm); Z axis, fluorescence intensity (A.U., arbitrary units).
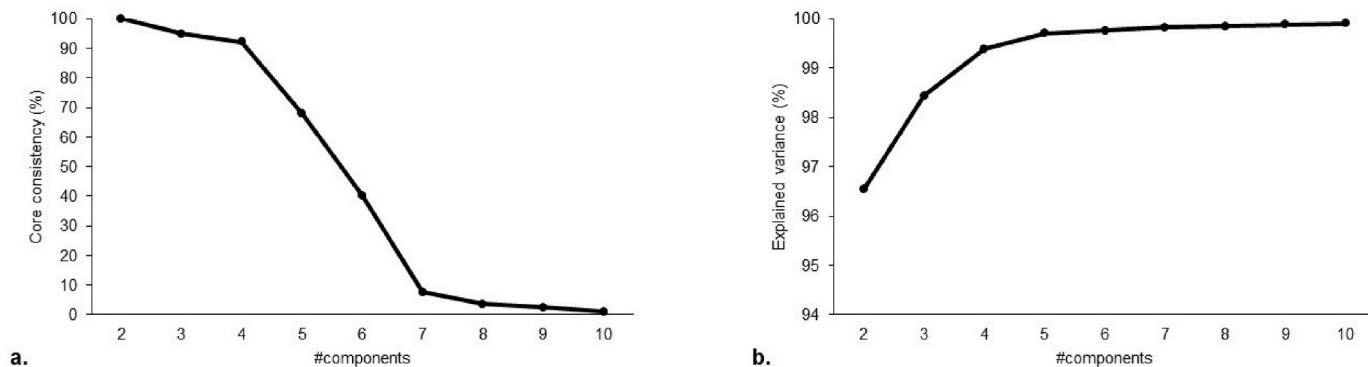

Fig. 2. Core consistency (a) and percentage of explained variance (b) of PARAFAC models from 2 to 10 components, built on the overall averaged dataset of EEM recorded from 15 different edible insect powders.
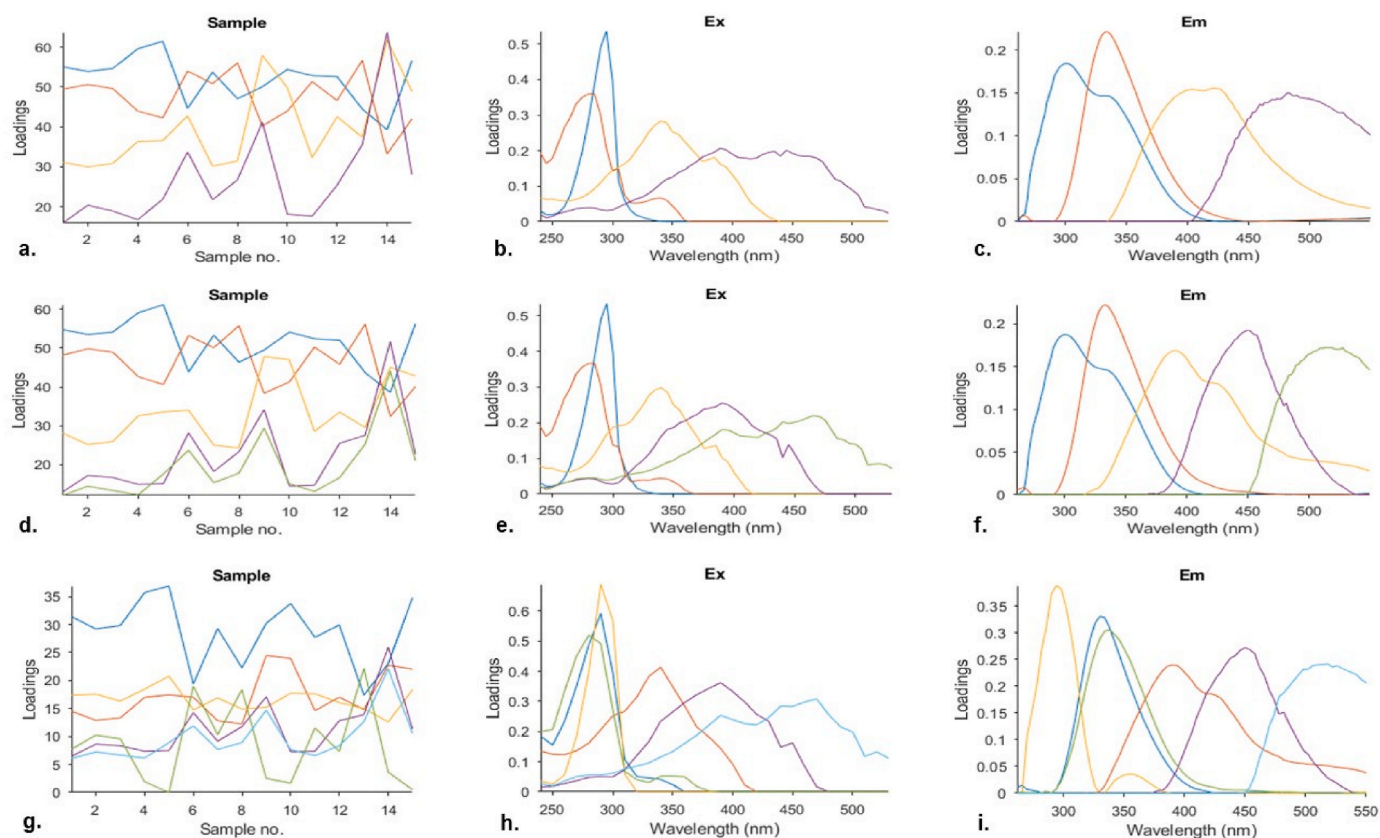
Fig. 3. Loadings of PARAFAC models 4, 5, 6 computed on the overall averaged insect EEM: model-4 (sample mode: a; excitation mode: b; emission mode: c), model-5 (sample mode: d; excitation mode: e; emission mode: f) and model-6 (sample mode: g; excitation mode: h; emission mode: i).

could be observed in models 4 and 5 (Fig. 3b, c, 3e, 3f). Additionally, model-5 (Fig. 3e and f) showed clear peak at excitation 390 nm and emission 450 nm (component violet). The same component was also detected in model-4; however in this model, it displayed a broader range of excitation, with maximum at 390 nm and shoulder between 430 nm and 470 nm, while the emission was ranged between 458 and 527 nm. A further component (green) with excitation maxima at 465 nm and shoulders at 390 nm and 520 nm, corresponding with emission ranged between 504 nm and 527 nm was observed in model-5. In PARAFAC model-6 (Fig. 4h and i), the first component ($\lambda_{ex/em}$: 295/300 nm with shoulder at 333 nm) detected in the models 4 and 5 was divided into two different components: yellow ($\lambda_{ex/em}$: 295/300 nm) and blue components ($\lambda_{ex/em}$: 295/330 nm), the latest representing the shoulder associated with the first component of models 4 and 5.

PARAFAC model-5 was optimised and validated after increasing the convergence criteria to 10^{-10}. PARAFAC models with five components were also validated for each species, and the peaks position was confirmed on the intraspecies datasets, although slight differences were observed on the excitation maximum of components one ($\lambda_{ex} = 275$ nm), four ($\lambda_{ex} = 385$ nm), five ($\lambda_{ex} = 465$ nm) for *Gryllus assimilis*, one ($\lambda_{ex} = 280$ nm), three ($\lambda_{ex} = 345$ nm), five ($\lambda_{ex} = 470$ nm) for *Gryllus bimaculatus* and on the emission maximum of several components among the considered species (Table 3).

3.3. Peak identification

Emission spectra recorded at the maximum of the absorption band (maximum excitation wavelength) of the analysed standard substances are displayed in Fig. 4. Several pure compounds and mixtures showed fluorescence peaks at excitation wavelengths ranging between 280 and 295 nm (tyrosine, tryptophan, tocopherol, albumin and mixtures of: tryptophan + tocopherol, tyrosine + tocopherol, tryptophan + tyrosine

+ tocopherol) and might be therefore suitable for explaining the first two PARAFAC components. Similarly, PARAFAC component-3 ($\lambda_{ex} = 340$ nm) might be associated to pyridoxine, NADH, pterins and collagen. PARAFAC model-5 run on the overall averaged dataset was significantly improved when pure spectra of these compounds were added (Fig. 5).

Comparison between PARAFAC components and pure standard spectra showed good correspondence between component-1 and mixture of tocopherol, tryptophan and tyrosine (Fig. 6a), component-2 and albumin (Fig. 6b), component-3 and collagen, pyridoxine and pterins (Fig. 6c).

4. Discussion

To the best of our knowledge, this study represents the first investigation of the fluorescence landscape of edible insects. Although insect fluorescence has been largely explored, most of the studies investigated live insects and fluorescence phenomena connected with pigments responsible for their colourful teguments (Lagorio et al., 2015; Welch et al., 2012).

In the present work, EEMs of powders from 5 different edible insect species and 3 different origins were recorded and characterised. High complexity of their fluorescence landscape was observed, suggesting that edible insects are chemically complex matrices. Indeed, PARAFAC analysis conducted on the overall averaged dataset was validated for five components, indicating that five different peaks could be detected on the analysed EEM. This is in line with other traditional food such as meat, cheese and fish, where 4 or 5 fluorescence peaks are usually described (Andersen and Mortensen, 2008; Christensen et al., 2006; Islam et al., 2020).

Additionally, the five picked PARAFAC components were also detected on the intraspecies datasets, implying that fluorescence of several Orthoptera species raised from the same compounds. However,
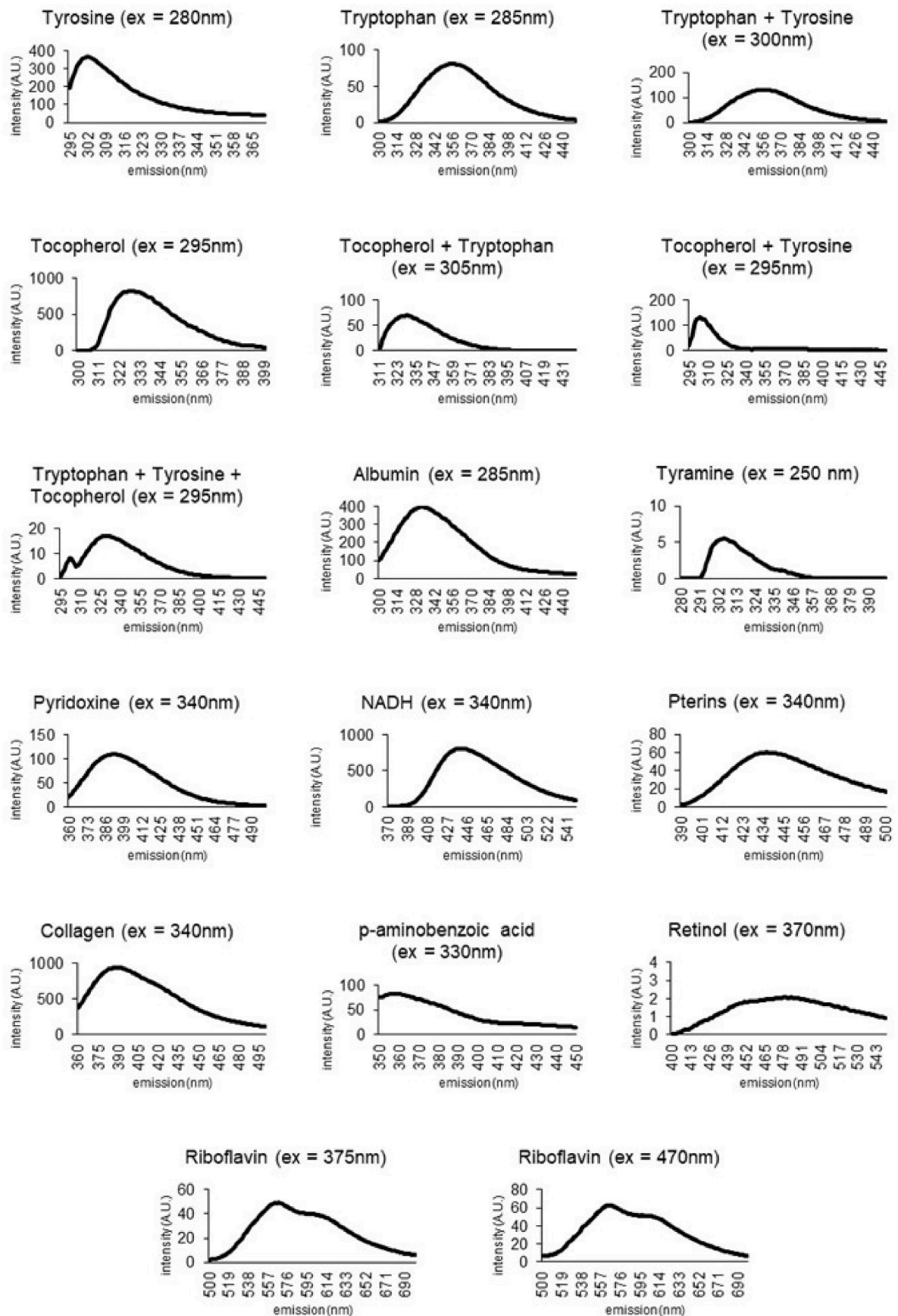
Fig. 4. Emission spectra of the standard pure compounds and mixtures recorded at their maximum absorption band (ex).

Table 3
Excitation and Emission maxima of the validated PARAFAC model on the overall averaged dataset and intraspecies datasets.

Dataset	PARAFAC model (Comp.)	Comp. 1 ($\lambda_{ex/em}$; nm)	Comp. 2 ($\lambda_{ex/em}$; nm)	Comp. 3 ($\lambda_{ex/em}$; nm)	Comp. 4 ($\lambda_{ex/em}$; nm)	Comp. 5 ($\lambda_{ex/em}$; nm)
overall	5	295/300; 333	285/333	340/392; 420	390/450	465/504-527
A. domesticus	5	295/299; 331	285/333	340/389; 425	390/452–457; 481	470/484-527
G. assimilis	5	295/302; 333	275/333	340/385; 422	385/443	465/484-527
G. bimaculatus	5	295/302; 335	280/334	345/392; 425-430	400/458	470/484-527
L. migratoria	5	295/299; 331	285/332	340/392; 425	390/457-481	470/504-540
S. gregaria	5	295/299; 340	285/332	340/391; 420	390/444-453	470/514-540

slight differences between samples could still be detected. Such differences were mainly due to the position of the emission maxima of each PARAFAC component, which may be attributed to different physio-chemical properties of the analysed powders. Indeed, it is well known that optical properties of each fluorophore depend on the environment where the specific fluorophore is located (Christensen et al., 2006). Furthermore, since several molecules may interact with the fluorophores (Sikorska et al., 2019), modifying their spectra, different chemical compositions of the analysed powders may lead to important differences in the peak position. This is relevant when different feeds are used for insect rearing as the diet has a strong impact on insect nutritional quality (Ojha et al., 2021; Van Huis et al., 2013). Therefore, if different feeds are provided to different insect species, fluorescence characterization and discrimination of insects as function of species and origin may be performed, as already shown on traditional products (Genis et al., 2019; Hammami et al., 2013; Lenhardt et al., 2017). However, since limited dataset was used in this experiment and the discrimination was not the object of this study, further and more focused research is needed in order to shed light on this aspect. Further differences between species and origins could also be highlighted on magnitude of the fluorescence peaks, which may be connected with different concentrations of the fluorophores in different samples. Indeed several studies have displayed that the PARAFAC loadings computed on sample mode pinpoint the relative concentration of the underlined fluorophore in each sample, allowing to use fluorescence for quantitative analysis (Bro, 1997; Sikorska et al., 2019). However, in order to implement fluorescence spectroscopy for chemical compounds quantification, characterisation of each fluorescence peak should be performed.

In the present study, identification of the compounds responsible for the fluorescence peaks was based on the idea that each PARAFAC component is associated with a specific chemical compound (Christensen et al., 2006; Murphy et al., 2013). Nevertheless, due to the high chemical complexity of edible insects (Rumpold and Schlueter, 2013), interaction between molecules can be expected, implicating that more compounds describe the same fluorescence peak.

Potential fluorophores responsible for edible insect fluorescence might be amino acids, vitamins, polyphenols, pigments and nucleic acid, which are the traditional fluorophores detected in food (Fernández-Romero and Aguilar-Caballos, 2019). Additionally, further compounds, such as purine and uric acid have been detected in some insect species (Melber and Schmidt, 1992; Mello and Vidal, 1985), therefore, they should be considered. In this study, the first two PARAFAC components exhibit excitation maximum at 285 and 295 nm, respectively. Proteins are usually excited in this region (Lakowicz, 2013). Edible insects are known to be a very important protein source, having concentrations ranging between 25 and 75% (Oonincx and Finke, 2020; Rumpold and Schlueter, 2013); therefore, it is possible to hypothesize that they are responsible for at least one fluorescence peak. Protein fluorescence origins from three aromatic amino acids, i.e. phenylalanine ($\lambda_{ex/em}$ = 260/282 nm), tyrosine ($\lambda_{ex/em}$ = 275/303 nm) and tryptophan ($\lambda_{ex/em}$ = 280/350 nm) (Lakowicz, 2013). Since proteins are usually excited at 280 nm, phenylalanine is not detected, while tryptophan and tyrosine could be detected in both, pure and combined forms. Therefore, PARAFAC component-2 (λ_{ex} = 285 nm) may be due to proteins. Specifically, perfect overlapping between this component and albumin spectra was

observed, therefore component-2 might be associated to albumin. However, since Montowska et al. (2019), studying the protein profile of cricket powders, did not report this specific protein, a mixture of several amino acids (i.e. tryptophan and tyrosine) may be a more suitable explanation for this peak. Indeed, tryptophan residues are usually located in the hydrophobic area of the proteins (Bussler et al., 2015) and such environment leads to a shift of their emission maximum from 350 to 320–330 nm (Albani, 2012), which is suitable for explaining the aforementioned PARAFAC component. Moreover, fluorescence peaks centred between 330 and 340 nm, detected in several other foods, such as fish and meat, are usually associated with this amino acid (Christensen et al., 2006). Nevertheless, since energy transfer from tyrosine to tryptophan is a common phenomenon happening within the proteins (Lakowicz, 2013), the aforementioned peak might also be the result of a mixture of tyrosine and tryptophan in hydrophobic environment.

Due to similar physical phenomenon, the PARAFAC component-1 (λ_{ex} = 295 nm) might also be associated with a mixture of tyrosine and tryptophan. However, since tyrosine cannot be excited at wavelengths higher than 290 nm (Lakowicz, 2013), it seems improbable that tyrosine is responsible for this fluorescence peak. Nevertheless, the detection of tyrosine at this wavelength cannot be excluded as an excitation slit width of 10 nm was used in this study, meaning that the excitation could fluctuate between 285 and 305 nm. Alternative explanation for the main component peak might be the Rayleigh or Raman scattering. A Raman effect was not observed due to the nature of samples (powder form) and it is typically due to absorption of solvents (Andrade-Eiroa et al., 2013). On the other hand, Rayleigh signal could be detected, even though preliminary correction was performed. Nevertheless, it might be excluded as it is usually beyond the measurement range of the instrument, while the studied peak is well defined. Therefore, the peak at emission 300 nm may be attributed to tyrosine. The shoulder at 333 nm is, instead, probably associated to tryptophan. However, excitation of 295 nm can also allow to detect tocopherol (i.e. vitamin E), which is an important fluorophore in several food products, such as milk, cheese, meat, oil, cereal flour and others (Altomonte et al., 2019; Christensen et al., 2006; Gherghina et al., 2021; Lenhardt et al., 2017). It shows a fluorescence peak centred at $\lambda_{ex/em}$ = 298/330 nm (Albani, 2012; Sikorska et al., 2019), therefore it can be expected to be co-responsible for this fluorescence peak.

PARAFAC component-3 was attributed to a mixture of pyridoxine, collagen and pterins. In particular, pterins, a class of chemical compounds responsible for pigmentation, nitrogen metabolisms, visual and neurohormonal activities (Ziegler and Harmsen, 1970), have been already detected in insects when emission spectra ranging between 420 and 455 nm over excitation 340 nm was considered (Abels and Ludescher, 2003; Bridges and Sohal, 1980; Kumazawa and Tabata, 2001; Melber and Schmidt, 1992). Pterins show a characteristic peak at $\lambda_{ex/em}$ = 350/450 nm (Lagorio et al., 2015); therefore, they can explain the shoulder of this PARAFAC component. However, since the same excitation wavelength has been used to detect NADH ($\lambda_{em,max}$ = 395 and 465 nm (Hassoun and Karoui, 2015; Sikorska, 2019)) in several food products (Christensen et al., 2006; Hassoun et al., 2020; Hassoun and Karoui, 2015; Sikorska, 2019; Sikorska et al., 2019), further analyses are requested in order to have a secure identification of the underlined peak. Other fluorophores usually detected in animal-derived food and able to
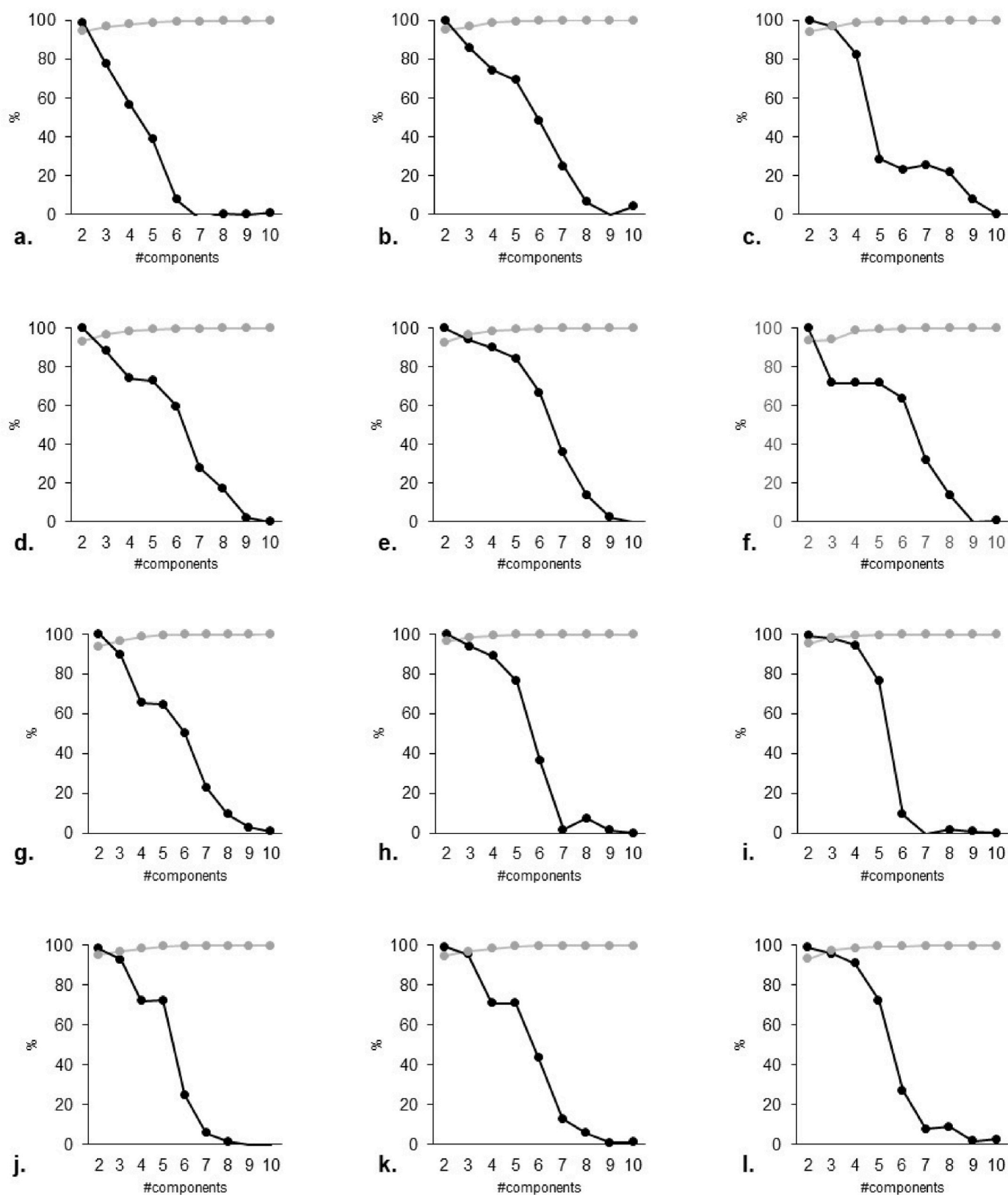
Fig. 5. Core consistency (black line) and percentage of explained variance (grey line) of PARAFAC analyses performed on the insect EEM after adding the EEM recorded from one single chemical standard compound (or mixture): tyrosine (a); tryptophan (b), tocopherol (c); tocopherol + tyrosine (d); tocopherol + tryptophan (e); tocopherol + tyrosine + tryptophan (f); tyrosine + tryptophan (g); albumin (h); collagen (i); NADH (j); pterins (k); pyridoxine (l).
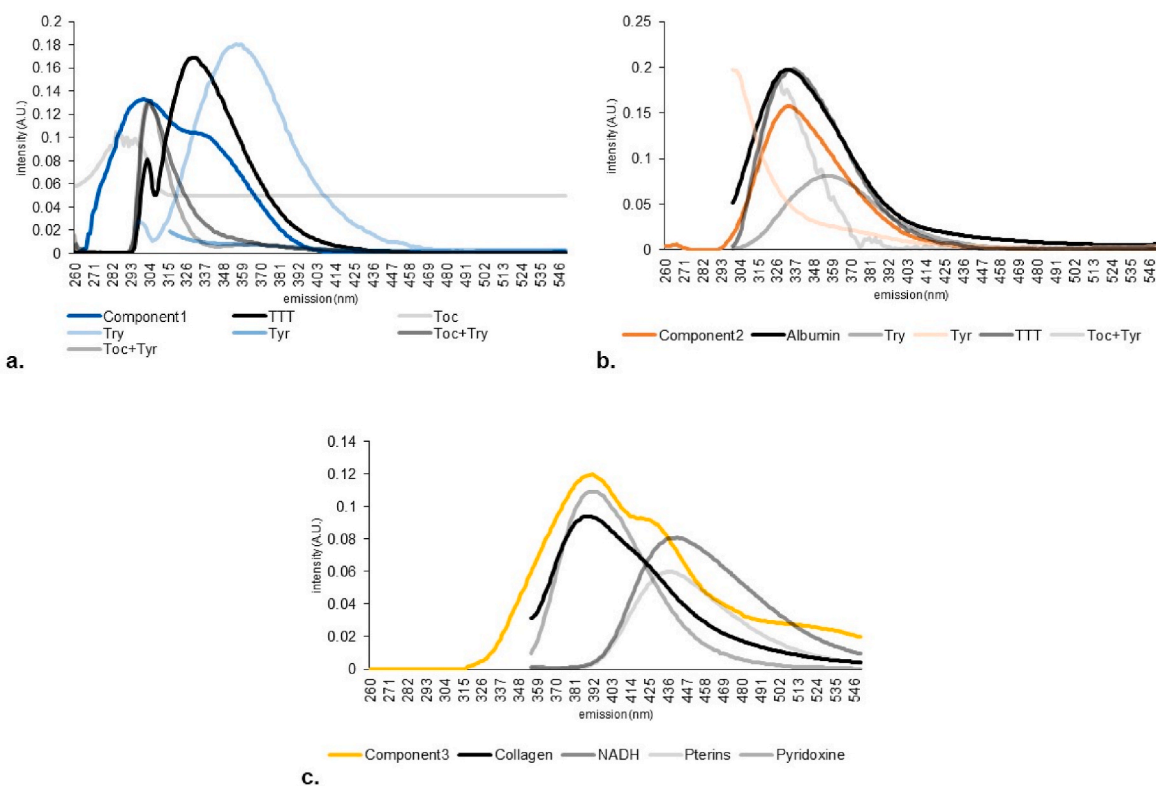
Fig. 6. Comparison between PARAFAC components 1, 2, 3 and spectra recorded from pure standard compounds. **a:** PARAFAC component-1, tocopherol + tyrosine + tryptophan (TTT), tocopherol (Toc), tryptophan (Try), tyrosine (Tyr), tocopherol + tryptophan (Toc + Try), tocopherol + tyrosine (Toc + Tyr). **b:** PARAFAC component-2, albumin, tryptophan (Try), tyrosine (Tyr), tocopherol + tyrosine + tryptophan (TTT), tocopherol + tyrosine (Toc + Tyr). **c:** PARAFAC component-3, collagen, NADH, pterins, pyridoxine.

emit fluorescence in the same region ($\lambda_{ex/em}$ = 350/420 nm) are represented by Schiff bases, originated through chemical reactions between saturated aldehydes and amino acids (Veberg et al., 2006). However, they are produced during the storage at high temperatures, and since the samples were stored for a short time at 4 °C, their presence can be excluded. Nevertheless, further analysis should be carried out in order to understand if such products can be used for monitoring storage time and conditions of edible insect powders. The main peak of the aforementioned PARAFAC component may instead be assigned to collagen ($\lambda_{ex/em}$ = 320/400 nm (Skjervold et al., 2003)) and/or pyridoxine ($\lambda_{ex/em}$ = 340/400 nm (Sikorska et al., 2004)). Pyridoxine (i.e. vitamin B6) is usually detected in high amounts in unprocessed insects (Oonincx and Finke, 2020) and displays strong fluorescence intensity, also if present in traces (Sikorska et al., 2004). Collagen is a structural protein, very common in animal tissue (Shoulders and Raines, 2009; Sutherland et al., 2013) and its fluorescence is often detected in meat (Christensen et al., 2006). Since the latter compound has been found in several insect species as well (Ashhurst, 1982; Ashhurst and Bailey, 1980; François, 1985), both pyridoxine and collagen are strong candidates for being described by the underlined PARAFAC component.

Due to the low signal/noise ratio recorded at excitation and emission higher than 400 and 450 nm, respectively, and to the high chemical complexity of this area, specific identification of the PARAFAC components 4 and 5 was not performed. However, since in the region where they were computed, vitamins (e.g. vitamin B2) and polyphenols (e.g. pherulic acid) (Ahmad et al., 2017; Christensen et al., 2005; Kahle et al., 2019; Yang et al., 2016) are usually detected, these peaks might be associated to mixtures of several vitamins and polyphenols. On the other hand, compounds potentially responsible for these two components may also be lipid oxidation products (Yamaki et al., 1992), already detected in meat and fish (Veberg et al., 2006). Therefore, in order to have an exact and punctual chemical identification of the latter two PARAFAC

components, further studies should focus on the fluorescence in the underlined region.

5. Conclusion

In the present study, the fluorescence landscapes of edible insects were investigated. PARAFAC analysis performed on EEM recorded from 15 insect powders was validated for five components suggesting that edible insect's optical fingerprint is characterised by five different peaks. The same PARAFAC components computed on the overall dataset were also detected in intraspecies dataset, pointing out that several insect powders have the same fluorophores. Slight differences in emission and excitation maxima, likely due to different feed and insect origin, could still be observed. Comparison between the PARAFAC components and emission spectra of standard compounds allowed to assign the first three components to mixture of tryptophan and tyrosine, mixture of tryptophan, tyrosine and tocopherol, mixture of pyridoxine, collagen and pterins, respectively.

In conclusion, this research shows that fluorescence spectroscopy can potentially be employed for fast monitoring of the composition of edible insects. However, further studies investigating other edible insect species and products thereof are needed in order to have a complete overview of the analytical potential of fluorescence in the edible insect sector.

the Horizon 2020 program. The authors declare no conflict of interest.

Declaration of competing interest

The authors declare that they have no known competing financial interests or personal relationships that could have appeared to influence the work reported in this paper.

References

Abels, J.P., Ludescher, R.D., 2003. Native fluorescence from juvenile stages of common food storage insects. J. Agric. Food Chem. 51 (3), 544–549. https://doi.org/10.1021/jf020775m.

Acković, L.L., Zeković, I., Dramićanin, T., Bro, R., Dramićanin, M.D., 2018. Modeling food fluorescence with PARAFAC. In: Reviews in Fluorescence 2017. Springer, Cham, pp. 161–197. https://doi.org/10.1007/978-3-030-01569-5_8.

Ahmad, M.H., Nache, M., Hitzmann, B., 2017. Potential of fluorescence spectroscopy in detection of low-levels of gluten in flour: a preliminary study. Food Control 73, 401–405. https://doi.org/10.1016/j.foodcont.2016.08.028.

Albani, J.R., 2012. Fluorescence spectroscopy in food analysis. Encyclopedia of Analytical Chemistry. https://doi.org/10.1002/9780470027318.a1011.pub2.

Altomonte, I., Conte, G., Serra, A., Mele, M., Cannizzo, L., Salari, F., Martini, M., 2019. Nutritional characteristics and volatile components of sheep milk products during two grazing seasons. Small Rumin. Res. 180, 41–49. https://doi.org/10.1016/j.smallrumres.2019.10.003.

Andersen, C.M., Bro, R., 2003. Practical aspects of PARAFAC modeling of fluorescence excitation-emission data. J. Chemometr. 17 (4), 200–215. https://doi.org/10.1002/cem.790.

Andersen, C.M., Mortensen, G., 2008. Fluorescence spectroscopy: a rapid tool for analyzing dairy products. J. Agric. Food Chem. 56 (3), 720–729. https://doi.org/10.1021/jf072025o.

Andrade-Eiroa, A., Canle, M., Cerda, V., 2013. Environmental applications of excitation-emission spectrofluorimetry: an in-depth review I. Appl. Spectrosc. Rev. 48 (1), 1–49. https://doi.org/10.1080/05704928.2012.692104.

Ashhurst, D.E., 1982. The structure and development of insect connective tissues. In: Insect Ultrastructure. Springer, Boston, MA, pp. 313–350. https://doi.org/10.1007/978-1-4615-7266-4_11.

Ashhurst, D.E., Bailey, A.J., 1980. Locust collagen: morphological and biochemical characterization. Eur. J. Biochem. 103 (1), 75–83. https://doi.org/10.1111/j.1432-1033.1980.tb04290.x.

Bertram, S.M., Rook, V., 2011. Jamaican field cricket mate attraction signals provide age cues. Ethology 117 (11), 1050–1055. https://doi.org/10.1111/j.1439-0310.2011.01958.x.

Bi, S.Y., Song, D.Q., Tian, Y., Zhou, X., Liu, Z.Y., Zhang, H.Q., 2005. Molecular spectroscopic study on the interaction of tetracyclines with serum albumins. Spectrochim. Acta Mol. Biomol. Spectrosc. 61 (4), 629–636. https://doi.org/10.1016/j.saa.2004.05.028.

Bosch, G., van Zanten, H.H.E., Zamprogna, A., Veenenbos, M., Meijer, N.P., van der Fels-Klerx, H.J., van Loon, J.J.A., 2019. Conversion of organic resources by black soldier fly larvae: legislation, efficiency and environmental impact. J. Clean. Prod. 222, 355–363. https://doi.org/10.1016/j.jclepro.2019.02.270.

Bridges, R.G., Sohal, R.S., 1980. Relationship between age-associated fluorescence and linoleic-acid in the housefly musca-domestica. Insect Biochem. 10 (5), 557–562. https://doi.org/10.1016/0020-1790(80)90091-8.

Bro, R., 1997. PARAFAC. Tutorial and applications. Chemometr. Intell. Lab. Syst. 38 (2), 149–171. https://doi.org/10.1016/S0169-7439(97)00032-4.

Bugden, J.B.C., Yeung, C.W., Kepkay, P.E., Lee, K., 2008. Application of ultraviolet fluorometry and excitation-emission matrix spectroscopy (EEMS) to fingerprint oil and chemically dispersed oil in seawater. Mar. Pollut. Bull. 56 (4), 677–685. https://doi.org/10.1016/j.marpolbul.2007.12.022.

Bussler, S., Steins, V., Ehlbeck, J., Schlueter, O., 2015. Impact of thermal treatment versus cold atmospheric plasma processing on the techno-functional protein properties from Pisum sativum 'Salamanca. J. Food Eng. 167, 166–174. https://doi.org/10.1016/j.jfoodeng.2015.05.036.

Christensen, J., Becker, E.M., Frederiksen, C.S., 2005. Fluorescence spectroscopy and PARAFAC in the analysis of yogurt. Chemometr. Intell. Lab. Syst. 75 (2), 201–208. https://doi.org/10.1016/j.chemolab.2004.07.007.

Christensen, J., Norgaard, L., Bro, R., Engelsen, S.B., 2006. Multivariate autofluorescence of intact food systems. Chem. Rev. 106 (6), 1979–1994. https://doi.org/10.1021/cr050019q.

Dufour, É., Frencia, J.P., Kane, E., 2003. Development of a rapid method based on front-face fluorescence spectroscopy for the monitoring of fish freshness. Food Res. Int. 36 (5), 415–423. https://doi.org/10.1016/S0963-9969(02)00174-6.

Duggan, D.E., Bowman, R.L., Brodie, B.B., Udenfriend, S., 1957. A spectrophotofluorometric study of compounds of biological interest. Arch. Biochem. Biophys. 68 (1), 1–14. https://doi.org/10.1016/0003-9861(57)90320-X.

Egelandsdal, B., Dingstad, G., Tøgersen, G., Lundby, F., Langsrud, Ø., 2005. Autofluorescence quantifies collagen in sausage batters with a large variation in myoglobin content. Meat Sci. 69 (1), 35–46. https://doi.org/10.1016/j.meatsci.2004.06.004.

Elcoroaristizabal, S., Bro, R., Garcia, J.A., Alonso, L., 2015. PARAFAC models of fluorescence data with scattering: a comparative study. Chemometr. Intell. Lab. Syst. 142, 124–130. https://doi.org/10.1016/j.chemolab.2015.01.017.

Fernández-Romero, J.M., Aguilar-Caballos, M.P., 2019. Fluorescence: food applications. Encyclopedia of Analytical Science, third ed. https://doi.org/10.1016/B978-0-12-409547-2.00156-6

François, J., 1985. The collagen of the Arthropoda. In: Biology of Invertebrate and Lower Vertebrate Collagens. Springer, Boston, MA, pp. 345–368. https://doi.org/10.1007/978-1-4684-7636-1_32.

Gasco, L., Biancarosa, I., Liland, N.S., 2020. From waste to feed: a review of recent knowledge on insects as producers of protein and fat for animal feeds. Current Opinion in Green and Sustainable Chemistry 23, 67–79. https://doi.org/10.1016/j.cogsc.2020.03.003.

Genis, D.O., Bilge, G., Sezer, B., Durna, S., Boyaci, I.H., 2019. Identification of cow, buffalo, goat and Ewe milk species in fermented dairy products using synchronous fluorescence spectroscopy. Food Chem. 284, 60–66. https://doi.org/10.1016/j.foodchem.2019.01.093.

Gherghina, E., Israel-Roming, F., Balan, D., Luta, G., Popa, A., Zachia, M., 2021. Assessment of vitamin content in different types of Romanian cheese. Romanian Biotechnological Letters 26 (2), 2375–2383. https://doi.org/10.25083/rbl/26.2/2375.2383.

Hammami, M., Dridi, S., Zaidi, F., Maamouri, O., Rouissi, H., Blecker, C., Karoui, R., 2013. Use of front-face fluorescence spectroscopy to differentiate sheep milks from different genotypes and feeding systems. Int. J. Food Prop. 16 (6), 1322–1338. https://doi.org/10.1080/10942912.2011.583706.

Hassoun, A., Carpena, M., Prieto, M.A., Simal-Gandara, J., Ozogul, F., Ozogul, Y., et al., 2020. Use of spectroscopic techniques to monitor changes in food quality during application of natural preservatives: a review. Antioxidants 9 (9). https://doi.org/10.3390/antiox9090882.

Hassoun, A., Karoui, R., 2015. Front-face fluorescence spectroscopy coupled with chemometric tools for monitoring fish freshness stored under different refrigerated conditions. Food Control 54, 240–249. https://doi.org/10.1016/j.foodcont.2015.01.042.

He, H.J., Sun, D.W., 2015. Microbial evaluation of raw and processed food products by Visible/Infrared, Raman and Fluorescence spectroscopy. Trends Food Sci. Technol. 46 (2), 199–210. https://doi.org/10.1016/j.tifs.2015.10.004.

Islam, K., Mahbub, S.B., Clement, S., Guller, A., Anwer, A.G., Goldys, E.M., 2020. Autofluorescence excitation-emission matrices as a quantitative tool for the assessment of meat quality. J. Biophot. 13 (1) https://doi.org/10.1002/jbio.201900237.

Kahle, E.M., Zarnkow, M., Jacob, F., 2019. Substances in beer that cause fluorescence: evaluating the qualitative and quantitative determination of these ingredients. Eur. Food Res. Technol. 245 (12), 2727–2737. https://doi.org/10.1007/s00217-019-03394-x.

Khan, S.I., Zamyadi, A., Rao, N.R.H., Li, X., Stuetz, R.M., Henderson, R.K., 2019. Fluorescence spectroscopic characterisation of algal organic matter: towards improved in situ fluorometer development. Environmental Science-Water Research & Technology 5 (2), 417–432. https://doi.org/10.1039/C8EW00731D.

Kumazawa, K., Tabata, H., 2001. A three-dimensional fluorescence analysis of the wings of male Morpho sulkowskyi and Papilio xuthus butterflies. Zool. Sci. 18 (8), 1073–1079. https://doi.org/10.2108/zsj.18.1073.

Lagorio, M.G., Cordon, G.B., Iriel, A., 2015. Reviewing the relevance of fluorescence in biological systems. Photochem. Photobiol. Sci. 14 (9), 1538–1559. https://doi.org/10.1039/c5pp00122f.

Lakowicz, J.R., 2013. Protein fluorescence. In: Principles of Fluorescence Spectroscopy. Springer science & business media. https://doi.org/10.1007/978-1-4615-7658-7_11.

Lawaetz, A.J., Stedmon, C.A., 2009. Fluorescence intensity calibration using the Raman scatter peak of water. Appl. Spectrosc. 63 (8), 936–940. Available at: https://www.osapublishing.org/as/abstract.cfm?URI=as-963-938-936.

Lenhardt, L., Bro, R., Zekovic, I., Dramicanin, T., Dramicanin, M.D., 2015. Fluorescence spectroscopy coupled with PARAFAC and PLS DA for characterization and classification of honey. Food Chem. 175, 284–291. https://doi.org/10.1016/j.foodchem.2014.11.162.

Lenhardt, L., Zekovic, I., Dramicanin, T., Milicevic, B., Burojevic, J., Dramicanin, M.D., 2017. Characterization of cereal flours by fluorescence spectroscopy coupled with PARAFAC. Food Chem. 229, 165–171. https://doi.org/10.1016/j.foodchem.2017.02.070.

Li, Y.S., Church, J.S., 2014. Raman spectroscopy in the analysis of food and pharmaceutical nanomaterials. J. Food Drug Anal. 22 (1), 29–48. https://doi.org/10.1016/j.jfda.2014.01.003.

Maeno, K.O., Piou, C., Ghaout, S., 2020. The desert locust, Schistocerca gregaria, plastically manipulates egg size by regulating both egg numbers and production rate according to population density. J. Insect Physiol. 122 https://doi.org/10.1016/j.jinsphys.2020.104020.

Melber, C., Schmidt, G.H., 1992. Identification of fluorescent compounds in certain species of Dysdercus and some of their mutants (Heteroptera: pyrrhocoridae). Comp. Biochem. Physiol. Part B: Comparative Biochemistry 101 (1–2), 115–133. https://doi.org/10.1016/0305-0491(92)90167-.

Mello, M.L.S., Vidal, B.D., 1985. Microspectrofluorimetry of the naturally fluorescent substances of the malpighian tubules of triatoma-infestans and panstrongylus-megistus. Acta Histochem. Cytoc. 18 (4), 365–373. https://doi.org/10.1267/ahc.18.365.

Millie, D.F., Schofield, O.M.E., Kirkpatrick, G.J., Johnsen, G., Evens, T.J., 2002. Using absorbance and fluorescence spectra to discriminate microalgae. Eur. J. Phycol. 37 (3), 313–322. https://doi.org/10.1017/S0967026202003700.

Moller, M., Denicola, A., 2002. Protein tryptophan accessibility studied by fluorescence quenching. Biochem. Mol. Biol. Educ. 30 (3), 175–178. https://doi.org/10.1002/bmb.2002.494030030035.

Montowska, M., Kowalczewski, P.L., Rybicka, I., Fornal, E., 2019. Nutritional value, protein and peptide composition of edible cricket powders. Food Chem. 289, 130–138. https://doi.org/10.1016/j.foodchem.2019.03.062.

Murphy, K.R., Stedmon, C.A., Graeber, D., Bro, R., 2013. Fluorescence spectroscopy and multi-way techniques. PARAFAC. Analytical Methods 5 (23), 6557–6566. https://doi.org/10.1039/C3AY41160E.

Ohno, T., 2002. Fluorescence inner-filtering correction for determining the humification index of dissolved organic matter. Environ. Sci. Technol. 36 (4), 742–746. https://doi.org/10.1021/es0155276.

Ojha, S., Bussler, S., Schlueter, O.K., 2020. Food waste valorisation and circular economy concepts in insect production and processing. Waste Manag. 118, 600–609. https://doi.org/10.1016/j.wasman.2020.09.010.

Ojha, S., Grune, T., Bekhit, A., Schlueter, O., 2021. Bioaccessibility of nutrients from edible insects. Current Opinion in Food Science.

Oonincx, D.G.A.B., Finke, M.D., 2020. Nutritional value of insects and ways to manipulate their composition. Journal of Insects as Food and Feed 1–22. https://doi.org/10.3920/JIFF2020.0050.

Oonincx, D.G.A.B., van Broekhoven, S., van Huis, A., van Loon, J.J.A., 2015. Feed conversion, survival and development, and composition of four insect species on diets composed of food by-products. PLoS One 10 (12). https://doi.org/10.1371/journal.pone.0144601.

Patra, D., 2003. Applications and new developments in fluorescence spectroscopic techniques for the analysis of polycyclic aromatic hydrocarbons. Appl. Spectrosc. Rev. 38 (2), 155–185. https://doi.org/10.1081/ASR-120021166.

Pinotti, L., Giromini, C., Ottoboni, M., Tretola, M., Marchis, D., 2019. Review: insects and former foodstuffs for upgrading food waste biomasses/streams to feed ingredients for farm animals. Animal 13 (7), 1365–1375. https://doi.org/10.1017/S1751731118003622.

Porep, J.U., Kammerer, D.R., Carle, R., 2015. On-line application of near infrared (NIR) spectroscopy in food production. Trends Food Sci. Technol. 46 (2), 211–230. https://doi.org/10.1016/j.tifs.2015.10.002.

Pourreza, N., Mirzajani, R., Burromandpiroze, J., 2017. Fluorescence detection of vitamin B12 in human plasma and urine samples using silver nanoparticles embedded in chitosan in micellar media. Analytical Methods 9 (27), 4052–4059. https://doi.org/10.1039/c7ay01297g.

Poveda, J.A., Prieto, M., Encinar, J.A., Gonzalez-Ros, J.M., Mateo, C.R., 2003. Intrinsic tyrosine fluorescence as a tool to study the interaction of the Shaker B "ball" peptide with anionic membranes. Biochemistry 42 (23), 7124–7132. https://doi.org/10.1021/bi027183h.

Rumpold, B.A., Schlueter, O.K., 2013. Nutritional composition and safety aspects of edible insects. Mol. Nutr. Food Res. 57 (5), 802–823. https://doi.org/10.1002/mnfr.201200735.

Shoulders, M.D., Raines, R.T., 2009. Collagen structure and stability. Annu. Rev. Biochem. 78, 929–958. https://doi.org/10.1146/annurev.biochem.77.032207.120833.

Sikorska, 2019. Fluorescence spectroscopy and chemometrics in analysis of beverages. In: Quality Control in the Beverage Industry, vol. 17. Academic Press, pp. 161–203. https://doi.org/10.1016/B978-0-12-816681-9.00005-9.

Sikorska, Gorecki, T., Khmelinskii, I.V., Sikorski, M., De Keukeleire, D., 2004. Fluorescence spectroscopy for characterization and differentiation of beers. J. Inst. Brew. 110 (4), 267–275. https://doi.org/10.1002/j.2050-0416.2004.tb00621.x.

Sikorska, Khmelinskii, I., Sikorski, M., 2019. Fluorescence spectroscopy and imaging instruments for food quality evaluation. In: Evaluation Technologies for Food Quality. Woodshed Publishing, pp. 491–533. https://doi.org/10.1016/B978-0-12-814217-2.00019-6.

Silva, S., Guedes, C., Rodrigues, S., Teixeira, A., 2020. Non-destructive imaging and spectroscopic techniques for assessment of carcass and meat quality in sheep and goats: a review. Foods 9 (8). https://doi.org/10.3390/foods9081074.

Skjervold, P.O., Taylor, R.G., Wold, J.P., Berge, P., Abouelkaram, S., Culioli, J., Dufour, E., 2003. Development of intrinsic fluorescent multispectral imagery specific for fat, connective tissue, and myofibers in meat. J. Food Sci. 68 (4), 1161–1168. https://doi.org/10.1111/j.1365-2621.2003.tb09618.x.

Song, M.H., Han, M.H., Kwak, K.W., Lee, S., Kim, E.S., Park, K.H., Choi, J.Y., 2016. Effect of different diets on growth and development of the two-spotted cricket, Gryllus bimaculatus (Orthoptera: gryllidae). International Journal of Industrial Entomology 33 (2), 59–62. https://doi.org/10.7852/ijie.2016.33.2.59.

Stedmon, C.A., Bro, R., 2008. Characterizing dissolved organic matter fluorescence with parallel factor analysis: a tutorial. Limnol Oceanogr. Methods 6, 572–579. https://doi.org/10.4319/lom.2008.6.572.

Stedmon, C.A., Markager, S., 2005. Resolving the variability in dissolved organic matter fluorescence in a temperate estuary and its catchment using PARAFAC analysis. Limnol. Oceanogr. 50 (2), 686–697. https://doi.org/10.4319/lo.2005.50.2.0686.

Strasburg, G.M., Ludescher, R.D., 1995. Theory and applications of fluorescence spectroscopy in food research. Trends Food Sci. Technol. 6 (3), 69–75. https://doi.org/10.1016/S0924-2244(00)88966-9.

Sutherland, T.D., Peng, Y.Y., Trueman, H.E., Weisman, S., Okada, S., Walker, A.A., Ramshaw, J.A.M., 2013. A new class of animal collagen masquerading as an insect silk. Sci. Rep. 3 https://doi.org/10.1038/srep02864.

Tu, X., Zhang, Z., Johnson, D.L., Cao, G., Li, Z., Gao, S., Wang, G., 2012. Growth, development and daily change in body weight of Locusta migratoria manilensis (Orthoptera: acrididae) nymphs at different temperatures. J. Orthoptera Res. 21 (2), 133–140. https://doi.org/10.1665/034.021.0201.

Van Huis, A., Van Itterbeeck, J., Klunder, H., Mertens, E., Halloran, A., Muir, G., Vantomme, P., 2013. Edible insects: future prospects for food and feed security. FAO Forestry paper No 171, Available at: http://www.fao.org/3/i3253e/i3253e.pdf http://www.fao.org/3/i3253e/i3253e.pdf.

Veberg, A., Vogt, G., Wold, J.P., 2006. Fluorescence in aldehyde model systems related to lipid oxidation. Lwt-Food Science and Technology 39 (5), 562–570. https://doi.org/10.1016/j.lwt.2005.03.009.

Welch, V.L., Van Hooijdonk, E., Intrater, N., Vigneron, J.P., 2012. Fluorescence in insects. In: The Nature of Light: Light in Nature IV, vol. 8480. International Society for Optics and Photonics, p. 848004. https://doi.org/10.1117/12.929547.

Wunsch, U.J., Murphy, K.R., Stedmon, C.A., 2017. The one-sample PARAFAC approach reveals molecular size distributions of fluorescent components in dissolved organic matter. Environ. Sci. Technol. 51 (20), 11900–11908. https://doi.org/10.1021/acs.est.7b03260.

Yamaki, S., Kato, T., Kikugawa, K., 1992. Characteristics of fluorescence formed by the reaction of proteins with unsaturated aldehydes, possible degradation products of lipid radicals. Chem. Pharmaceut. Bull. 40 (8), 2138–2142. https://doi.org/10.1248/cpb.40.2138.

Yamashita, Y., Jaffe, R., Maie, N., Tanoue, E., 2008. Assessing the dynamics of dissolved organic matter (DOM) in coastal environments by excitation emission matrix fluorescence and parallel factor analysis (EEM-PARAFAC). Limnol. Oceanogr. 53 (5), 1900–1908. https://doi.org/10.4319/lo.2008.53.5.1900.

Yang, H., Xiao, X., Zhao, X., Hu, L., Lv, C., Yin, Z., 2016. Riboflavin and pyridoxine. In: Seventh International Symposium on Precision Mechanical Measurements, vol. 9903. International Society for Optics and Photonics, p. 99030H. https://doi.org/10.1117/12.2211248. Study on fluorescence spectra of thiamine, riboflavin and pyridoxine. In Seventh International Symposium on Precision Mechanical Measurements. International Society for Optics and Photonics, 9903.

Yang, H., Xiao, X., Zhao, X., Wu, Y., 2017. Intrinsic fluorescence spectra of tryptophan, tyrosine and phenyloalanine. In: Selected Papers of the Chinese Society for Optical Engineering Conferences Held October and November 2016. International Society for Optics and Photonics, p. 10255. https://doi.org/10.1117/12.2268397.

Zandomeneghi, M., Carbonaro, L., Caffarata, C., 2005. Fluorescence of vegetable oils: olive oils. J. Agric. Food Chem. 53 (3), 759–766. https://doi.org/10.1021/jf048742p.

Ziegler, I., Harmsen, R., 1970. The biology of pteridines in insects. Adv. Insect Physiol 6, 139–203. https://doi.org/10.1016/S0065-2806(08)60112-5.